Final Report:
Radio Frequency Noise Reduction in the LIGO Hanford Observatory

Matthew O. Withers
Department of Physics and Engineering
Washington and Lee University

Mentor: Dick Gustafson
Co-Mentor: Keita Kawabe

September 27, 2019

Introduction

In aLIGO, several critical subsystems, including the interferometer sensing and control (ISC) system and pre-stabilized laser (PSL), are dependent upon the reliable operation of a carefully designed radio frequency (RF) distribution system [1]. The RF distribution system produces and delivers a variety of RF signals, most derived from a base frequency of 9.10023 MHz [2]. These signals are used to both modulate and demodulate the interferometer's various input and output channels, making control of the interferometer possible. Given the RF distribution system's importance in the proper operation of aLIGO's interferometers, noise arising from its constituent components has the potential to increase the noise present in the interferometers' differential arm motion (DARM), the primary output used to detect gravitational waves. As such, developing a rigorous way to determine the effect of RF noise on DARM is of high value to continued efforts to fully characterize the behavior of the aLIGO detectors.

Our work at the LIGO Hanford Observatory (LHO) during the last month has focused on efforts to map the noise present in the shielding of LHO's RF transmission lines to DARM. By combining a theoretical description of the noise coupling mechanism with a series of experiments, we have produced plots describing the effect of the shield noise present on 9.10023 MHz, 45.50115 MHz, and 79.4 MHz cables on DARM. These plots allow us to evaluate the impact of shield noise on the behavior of the interferometer as a whole. Furthermore, the mapping procedure we have developed is transferable to investigations of other transmission lines used within the aLIGO interferometer network, making it of use in future efforts to identify noise within the RF distribution system.

aLIGO's RF Transmission Lines

Our efforts to map cable shield noise to DARM began with a brief background investigation of the types of RF transmission lines used at LHO. According to [3], the aLIGO detectors use HELIAX LDF4-50A cables, which are manufactured by Andrew. The specifications of these cables can be found at [4]. As a coaxial cable, LDF4-50A connects to an RF source and load as depicted in Figure 1. The RF signal V_S first passes from the source to the cable core, which

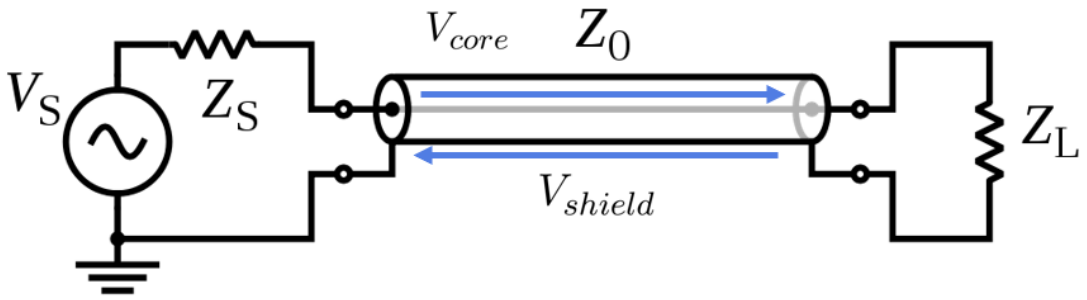

Figure 1: The typical connection configuration of a coaxial cable. V_S is the AC voltage signal provided to the cable, Z_S is the impedence of the signal source, Z_0 is the characteristic impedence of the cable, and Z_L is the impedance of the load. Notice that the AC signal travels through the core of the cable as V_{core}, while the shield (with voltage V_{shield}) provides a connection to ground.

delivers it to the load Z_L. After passing through the load, the signal returns to ground via the cable's shield, a conductive layer which surrounds the core. The shield also serves as a means

of protecting the core from unwanted electromagnetic interference (EMI) [5]. Thus, there are two primary voltage within the cable at any given time: the core voltage $V_{core} \approx V_S$ and the shield voltage $V_{shield} \approx V_S + Y$, where Y is the noise signal transferred to the shield via EMI. Our investigation focuses on determining how deviations of V_{shield} from V_{core} affect the DARM output of the LHO interferometer.

Noise Coupling Method

In March, LHO scientist Dr. Dick Gustafson, performed a series of RF noise injections onto the shielding of the main 9.10023 MHz transmission line, which is located in the CER at ISC-C4-41-5. He noticed that injections of $V_{inj} = -30$ dBV at a frequency $\nu_{inj} = 9.10023$ MHz $\pm Y$ Hz, appeared in DARM at Y Hz. Figure 2 shows the DARM signal resulting from an injection of $V_{inj} = -30$ dBV at $\nu_{inj} = 9.10023$ MHz $+ 55$ Hz, performed on 15/03/2019 at 20:50:40 UTC. Notice the presence of a noise line at 55 Hz in the H1 live trace (red curve) but

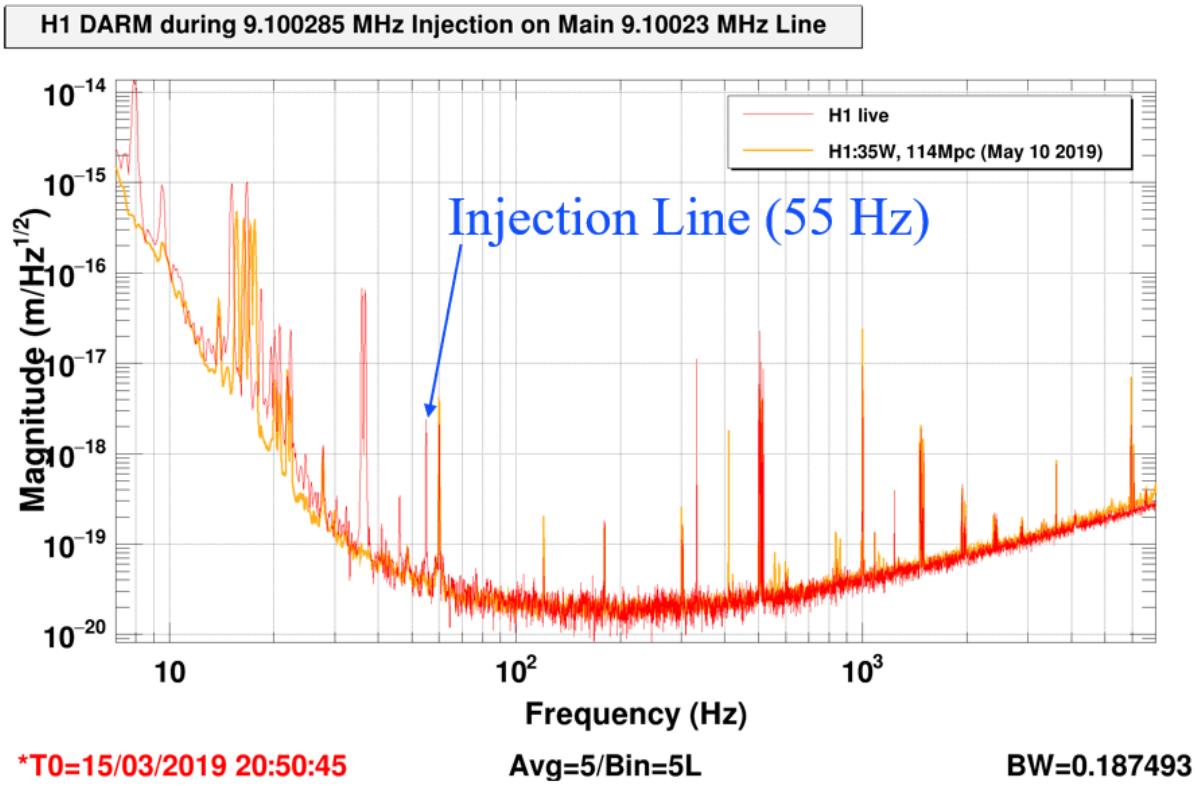

Figure 2: An amplitude spectral density plot of LHO's DARM signal (red curve) during a $\nu_{inj} = -30$ dBV, $V_{inj} = 9.10023$ MHz + 55 Hz injection onto the main 9.10023 MHz line. Notice that a line appears in the DARM at 55 Hz. This line is not present on LHO's reference DARM signal (yellow curve), collected on 10 May 2019, indicating that its presence is due to the injection.

not in the reference trace (yellow curve), indicating that it arose due to the injection. Because the noise line appears in DARM at a predictable location (i.e., at Y Hz when the injection is performed at 9.10023 MHz $\pm\, Y$ Hz), it characteristics can be used to map the noise present on the shield of the cable to DARM. Such mappings operate under the assumption that the transfer function from cable shield noise to DARM is flat. Such an assumption is a reasonable first step

given our observations; however, further work is necessary to verify the transfer function's true characteristics.

Shield Noise to DARM Mapping Methodology

There are two primary means of interacting with the shield of an RF cable: injection and probing. As Figure 3 demonstrates, an RF signal can be injected onto the shield of an RF transmission line via a 1:1 ferrite-core transformer. When such an injection occurs, a portion of

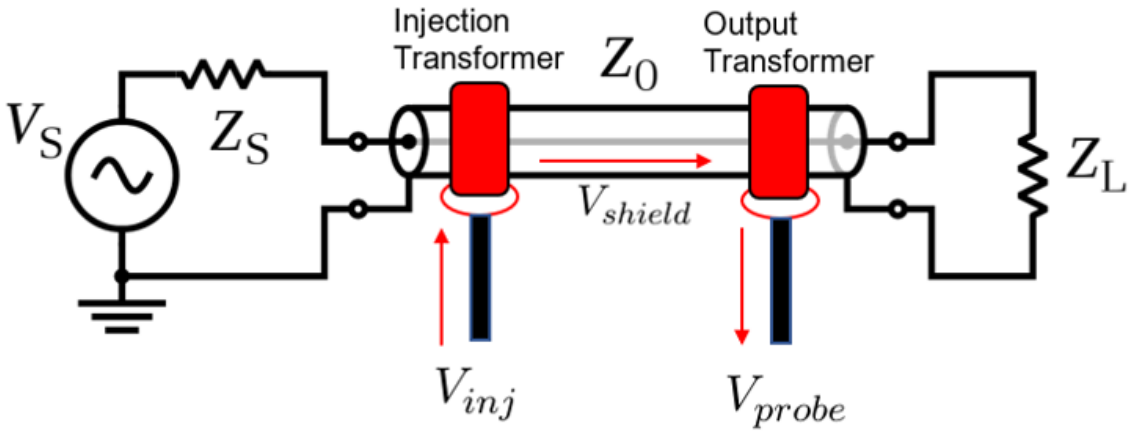

Figure 3: The typical setup for injecting signals onto the shield of an RF transmission line and probing the noise signal currently present on the line. The injection and output transformers are 1:1 ferrite-core transformers. Different configurations of these transformers allow for different measurements.

the injected signal V_{inj} passes to the cable shield as V_{shield}. For simplicity, we assumed a linear relationship between V_{shield} and V_{inj}. This produces the equation

$$V_{shield} = aV_{inj}. \tag{1}$$

Likewise, a 1:1 ferrite-core transformer can be used to probe the signal on the shield. We assumed that the probe output V_{probe} is also linearly related to V_{shield}. Thus, V_{probe} is given by

$$V_{probe} = bV_{shield}. \tag{2}$$

Using Equations 1 and 2, we found that the transfer function between V_{inj} and V_{probe} is simply

$$ab = \frac{V_{probe}}{V_{inj}}. \tag{3}$$

Next, we turned our attention to the relationship between cable noise and DARM. If the DARM response of an aLIGO interferometer is truly influenced by the noise present on the shield of an RF transmission line, the following relationship must hold:

$$\frac{\mathrm{ASD}(D)}{\mathrm{ASD}(V_{shield})} = \frac{D_{inj}}{V_{shield,inj}}, \tag{4}$$

where ASD(D) is the amplitude spectral density of mirror displacement in the interferometer (i.e., the classic DARM output in units of m/$\sqrt{\text{Hz}}$), ASD(V_{shield}) is the amplitude spectral density of the RF noise present on the cable shield (in units of V/$\sqrt{\text{Hz}}$), D_{inj} is the apparent mirror displacement caused by a controlled injection onto the cable shield (in units of m), and $V_{shield,inj}$ is the noise present on the shield due to that injection (in units of V). In other words, the effect of noise present on a cable's shield due to a test injection on the apparent mirror displacement should be equivalent to the effect of the amplitude spectral density of cable shield noise on the apparent amplitude spectral density of mirror displacement (DARM). Via algebraic manipulation and careful substitution of Equations 1 and 2, Equation 4 becomes

$$\text{ASD}(D) = \frac{1}{ab}\frac{D_{inj}}{V_{inj}}\text{ASD}(V_{probe}). \tag{5}$$

This equation suggests that, to map cable shield noise to DARM, we must have three pieces of information: the transfer function ab between V_{probe} and V_{inj} for a HELIAX LDF4-50A cable, the mirror displacement D_{inj} caused by an injected RF signal V_{inj}, and the amplitude spectral desnity of the noise on the cable ASD(V_{probe}). Therefore, we continued by conducting individual experiments to obtain each of these quantities.

Experiment 1: Obtaining the Cable Transfer Function *ab*

To obtain the transfer function ab we began by constructing the experimental apparatus outlined in Figure 4. Using the signal generator and a 1:1 ferrite-core transformer, we injected

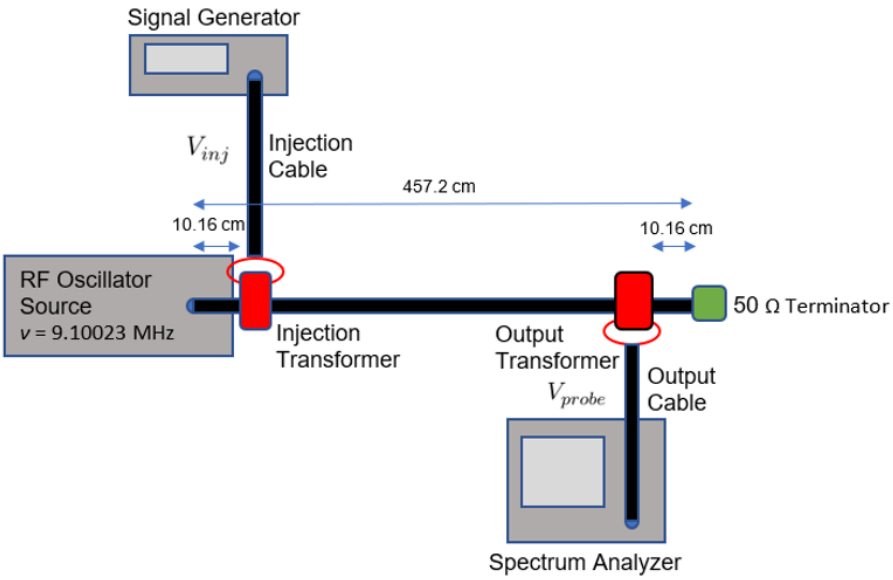

Figure 4: Our experimental setup for Experiment 1. The signal generator injects a noise signal V_{inj} onto the shield of the cable via a 1:1 ferrite-core transformer while the spectrum analyzer measures the noise level at the other end of the cable V_{probe} via another 1:1 ferrite-core transformer. Plotting V_{probe} versus V_{inj} allows me to determine the cable's transfer function ab.

a 9.10023 MHz + 5 Hz RF signal onto the cable shield at a variety of amplitudes, ranging from V_{inj} = 0.007 V to V_{inj} = 1.259 V. The injection frequency was selected to be the same frequency used during Experiment 2 (see below). Consistency between the injection frequency used here for cable characterization and the frequency in Experiment 2 for injection onto the

IFO's 9.10023 MHz cable is necessary because preliminary experiments demonstrated that the transfer function of HELIAX LDF4-50A changes according to the injection frequency. For each injected signal, we recorded the corresponding output V_{probe} at the other end of the cable by observing its amplitude on a spectrum analyzer. After plotting the V_{probe} series against the V_{inj}, we performed a least squares regression between the two series. The slope of the resulting linear equation is equivalent to the transfer function ab. Figure 5 demonstrates our results. The

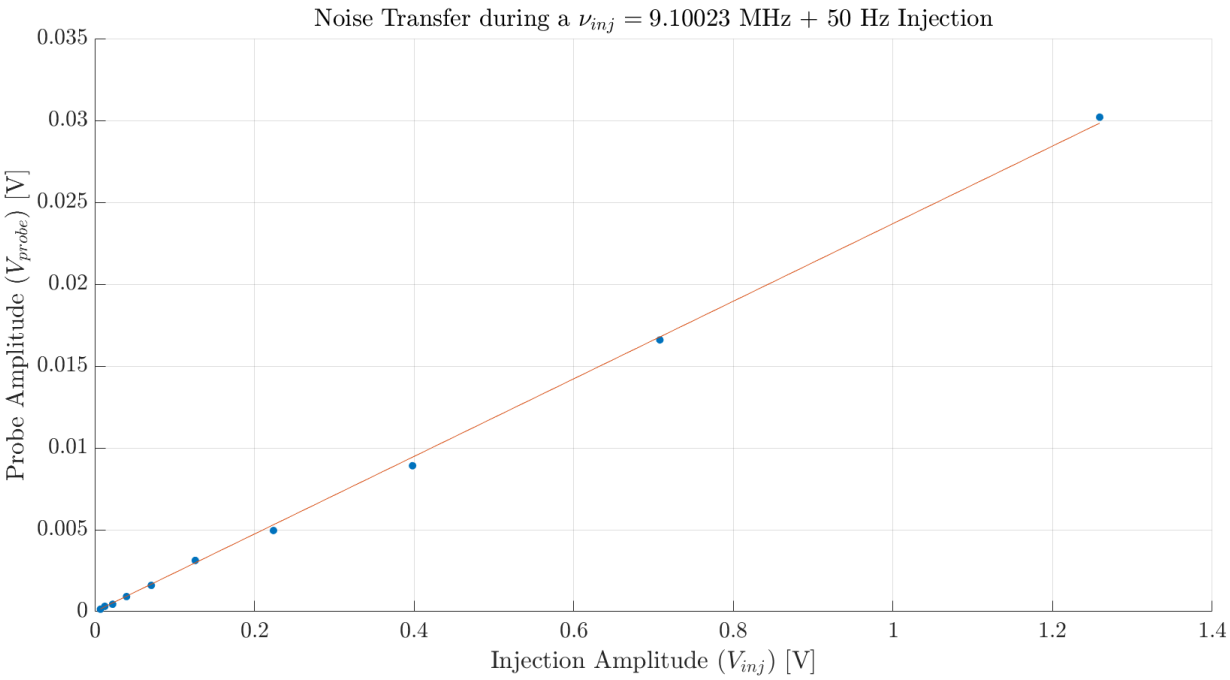

Figure 5: A plot of V_{probe} versus V_{inj} for our sample HELIAX LDF4-50A cable. The slope of the resulting curve provides the cable's transfer function ab under an injection at 9.10023 MHz + 50 Hz.

graph suggests that $ab = 0.0237$; therefore, we used this value throughout the remainder of our analysis.

Experiment 2: Obtaining the Apparent Displacement D_{inj} Produced by an Injection V_{inj}

To obtain the displacement D_{inj} produced by an injected frequency V_{inj}, we performed a ferrite-core transformer injection onto LHO's main 9.10023 MHz line (ISC-C4-41-5). Figure 6 details our experimental setup. Notice that we placed the injection transformer just before the transmission cable leaves the CER for the interferometer (i.e., at the outgoing patch pannel). Also notice that our injection frequency, ν_{inj} = 9.10023 MHz + 50 Hz, was offset 50 Hz from the cable's internal (core) frequency, which should produce a noise line at 50 Hz in DARM.

Figure 7 shows the DARM output at the time of the injection (red curve) along with an observing mode reference trace (yellow curve). Notice that a noise line is present at 50 Hz on the injection trace but not the observing mode trace, indicating that its presence is most likely due to the injection. To obtain D_{inj} from this plot of ASD(D_{inj}) we had to calculate the area under the 50 Hz peak. Figure 8 shows the peak in more detail. The peak is formed by several

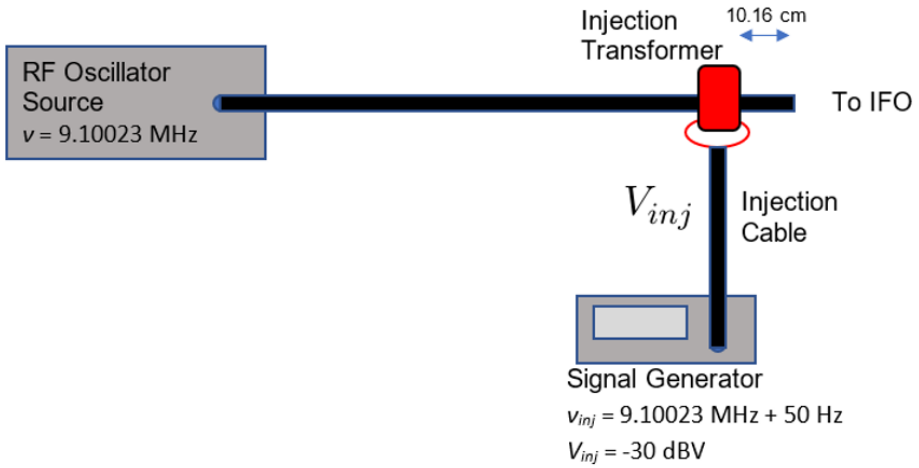

Figure 6: Our experimental setup for Experiment 2. The signal generator provides a $V_{inj} = -30$ dBV signal at $\nu_{inj} = 9.10023$ MHz + 50 Hz to the cable shield by passing the signal through a 1:1 ferrite-core transformer.

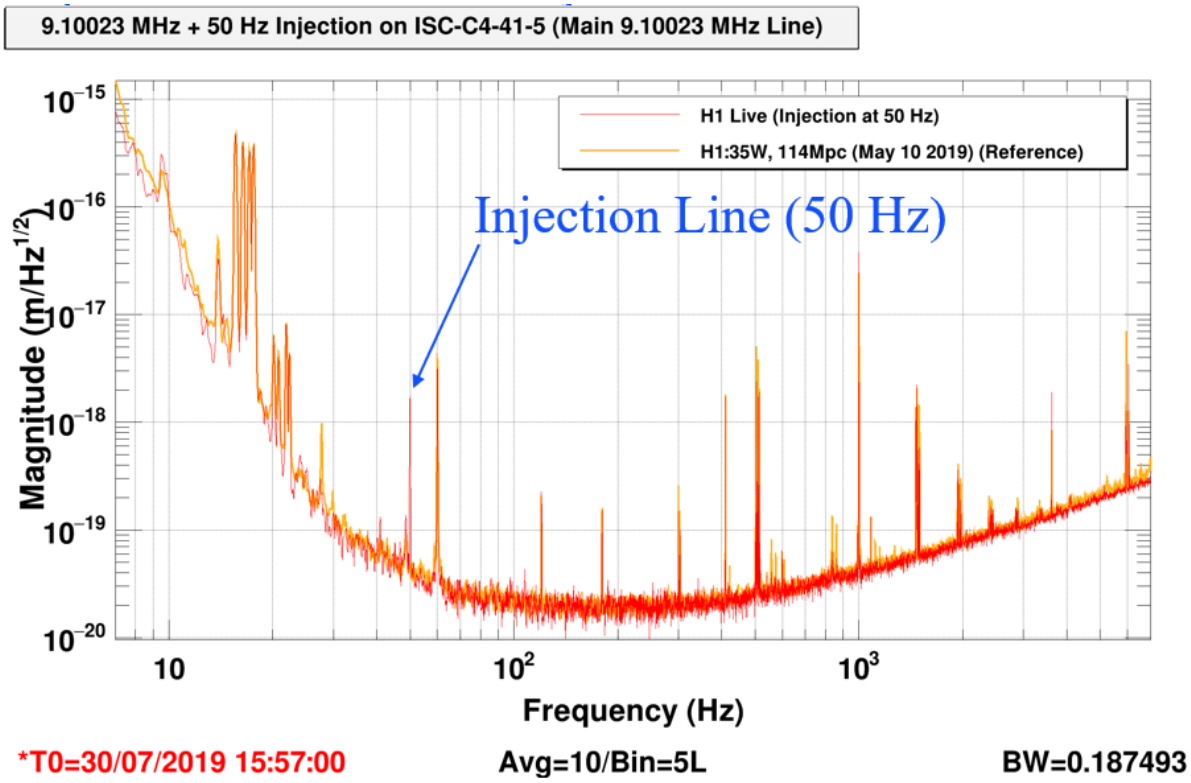

Figure 7: An amplitude spectral density plot of LHO's DARM signal (red curve) during a $V_{inj} = -30$ dBV at $\nu_{inj} = 9.10023$ MHz + 50 Hz injection onto the main 9.10023 MHz line. Notice that a line appears in the DARM at 50 Hz. This line is not present on LHO's reference DARM signal (yellow curve), collected on 10 May 2019, indicating that its presence is due to the injection.

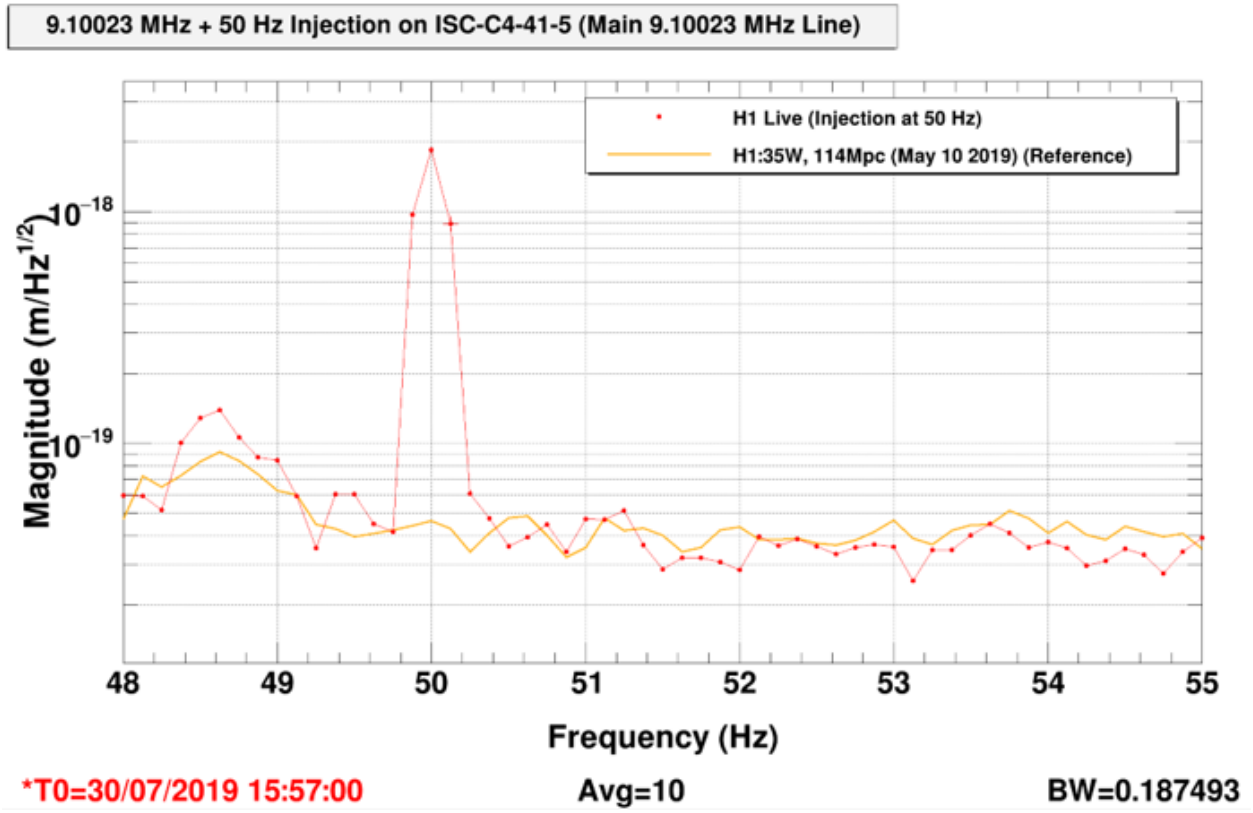

Figure 8: A close up view of the 50 Hz peak which arose during our injection (red curve). The apparent mirror displacement D_{inj} this peak represents is computed by calculating the area under the peak. Once again, notice the lack of a peak in the 10 May 2019 reference (yellow curve).

measurement bins d_i, which enclose an area

$$D_{inj} = \sqrt{\left(\sum_i d_i^2\right) BW}, \tag{6}$$

where BW is the measurement bandwidth. Using this equation, our data show that a $V_{inj} = -30$ dBV injection produces a displacement of $D_{inj} = 5.77 * 10^{-19}$ m.

Experiment 3: ASD(V_{probe}) Profile Collection

Finally, to obtain the ASD(V_{probe}) profile of the cable, we constructed the experimental apparatus shown in Figure 9. Notice that the output transformer, used along with the spectrum analyzer to measure V_{probe}, was located at the exact same location as the input transformer used in Experiment 2. This parallel was by design: we needed to know how noise at this location affects the DARM, given the reference provided by the injections performed during Experiment 2.

Figure 10 shows V_{probe} as measured by the spectrum analyzer[1]. Notice the peak at 9.10023 MHz, the frequency carried by the cable's core. Because analysis of previous RF noise injections indicates that a cable shield noise signal at 9.10023 MHz $\pm$ Y Hz appears in DARM at Y Hz,

[1]Note that the noise floor of the data in this image is limited by the noise floor of the spectrum analyzer. It is possible that more distinct signals exist; however, a device with a lower noise floor must be used to detect them.

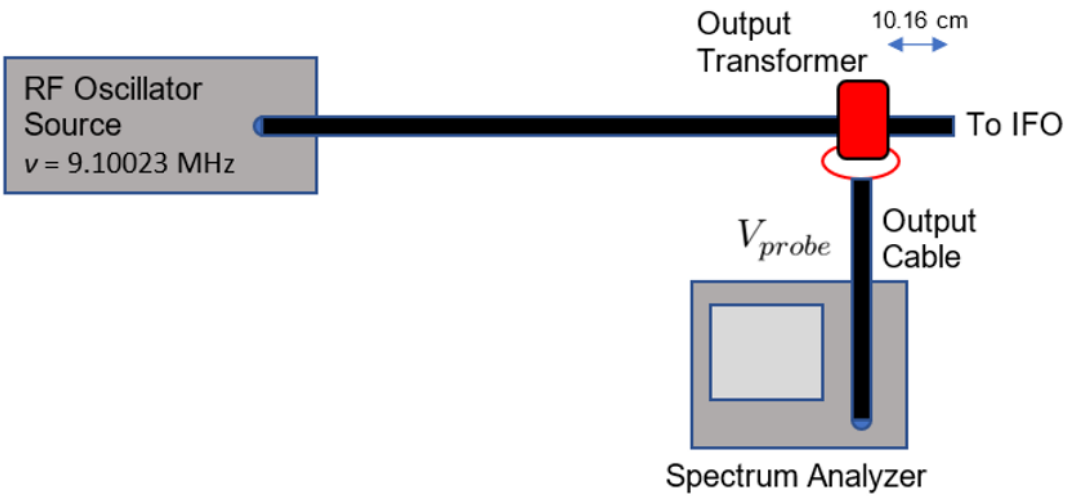

Figure 9: Our experimental setup for Experiment 3. The spectrum analyzer displays and records a profile of V_{probe}, which is collected from the cable's shield via a 1:1 ferrite core transformer.

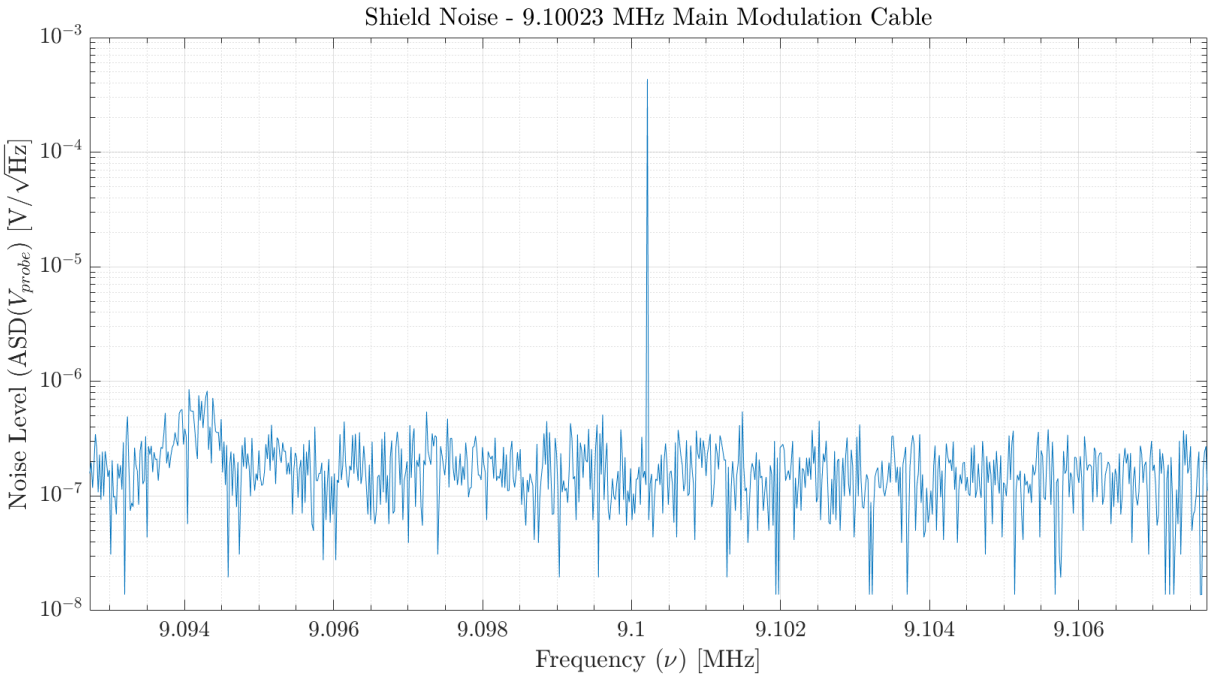

Figure 10: The spectrum of V_{probe}, collected via a spectrum anlayzer and a 1:1 ferrite-core transformer. Notice the presence of a peak at the cable's core frequency $\nu_{core} = 9.10023$ MHz (as expected). Any noise signal present at $\pm Y$ Hz of this peak will appear in LHO's frequency range at Y Hz. Note that the noise floor of the data is limited by the analyzer's noise floor.

we shifted the plot so that the 9.10023 MHz peak corresponds with 0 Hz (see Figure 11). To account for the fact that frequency offsets in the negative direction affect DARM in the same way as frequency offsets in the positive direction, we then folded the negative frequency values over the V_{probe}-axis (see Figure 12) and summed the overlapping series in quadrature (see

Figure 13). With this plot, which we expressed as an amplitude spectral density so as to obtain ASD(V_{probe}), we could then produce a map of the effect the main 9.20023 MHz cable has on aLIGO DARM.

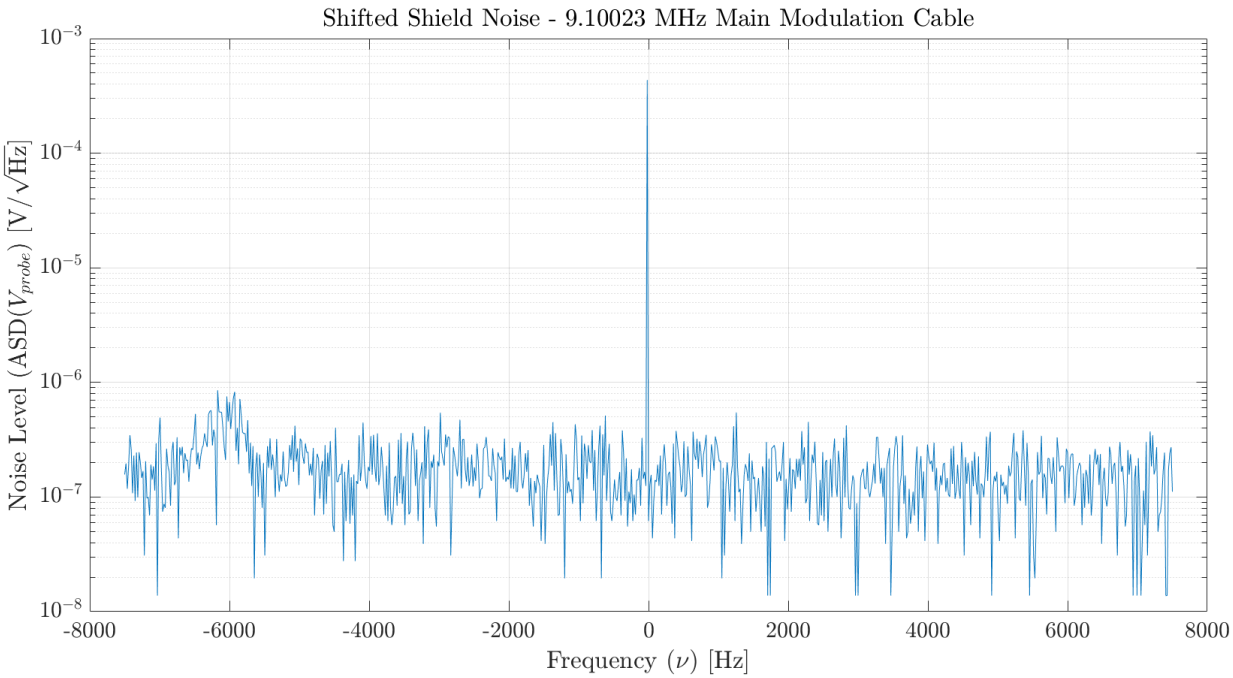

Figure 11: The spectrum of V_{probe} with the 9.10023 MHz peak shifted to $\nu_{probe} = 0$ Hz. Shifting the curve facilitates the mapping of noise frequencies to the proper location within LHO's frequency band.

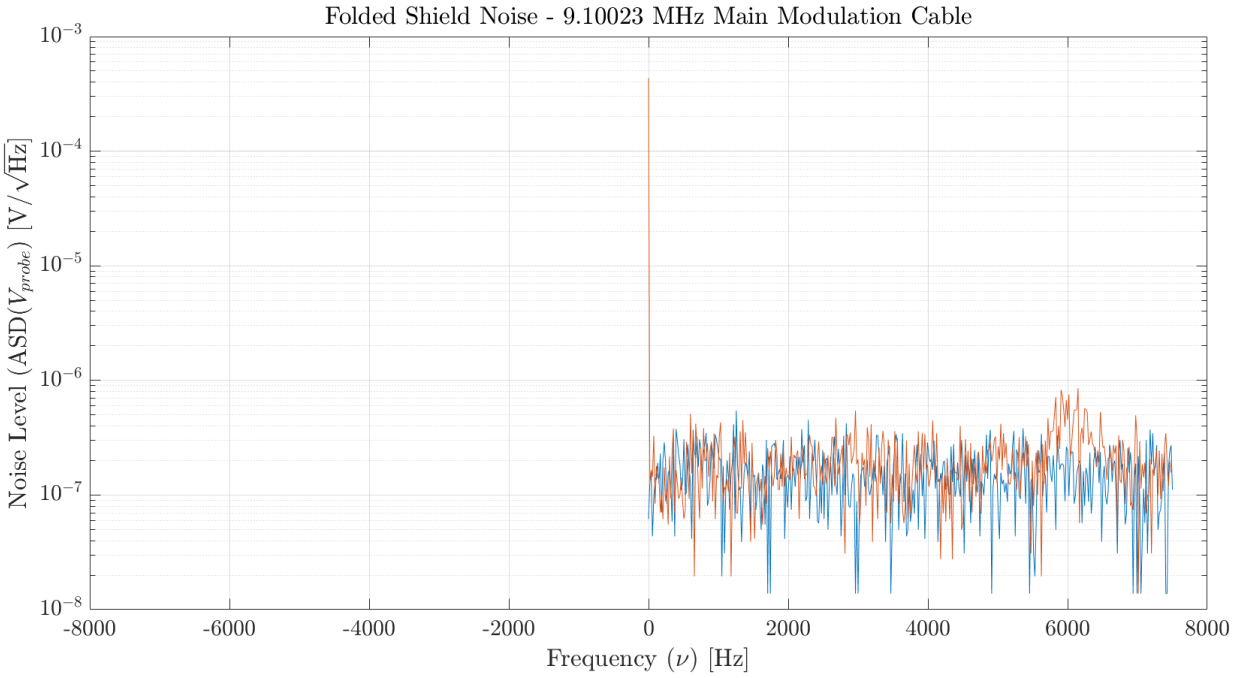

Figure 12: The spectrum of the shifted version of V_{probe} with all negative frequency values folded over the V_{probe}-axis. Folding occurs so as to match frequency values that are offset by $-Y$ Hz with frequency values that are offset by $+Y$ Hz.

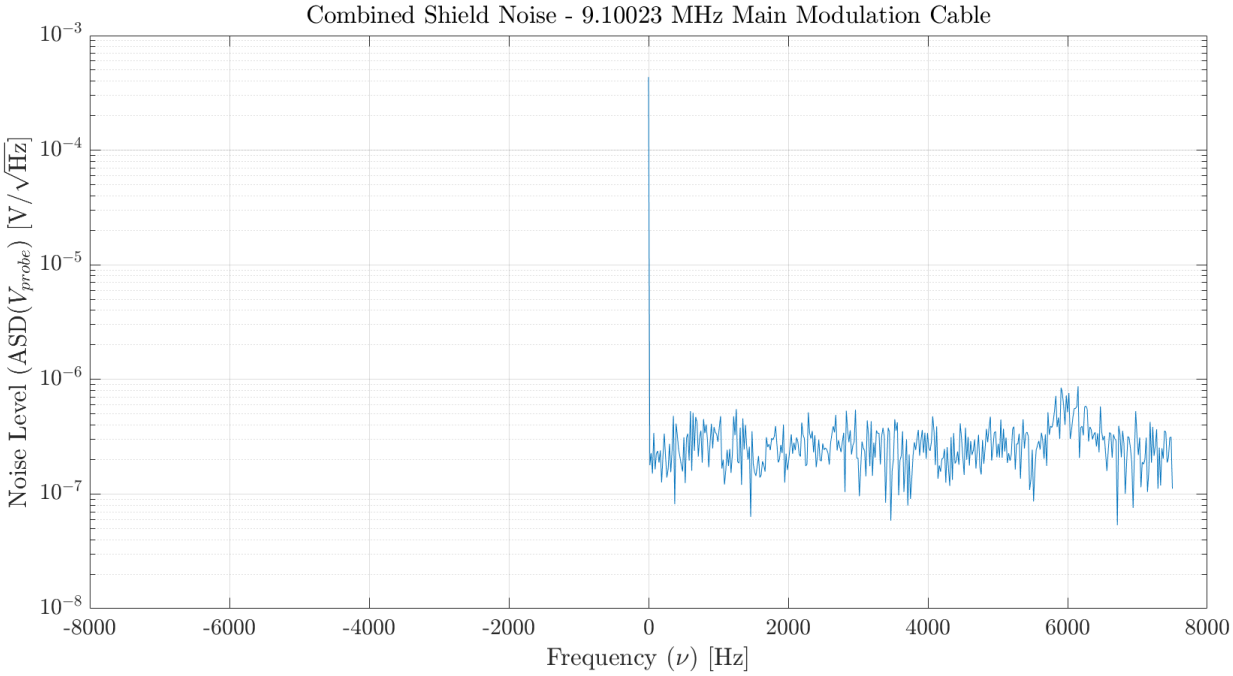

Figure 13: A plot of ASD(V_{probe}) after adding the folded portion of the V_{probe} probe spectrum to the unfolded section in quadrature and converting to an amplitude spectral density. This is the curve we ultimately passed into Equation 5 along with the results of Experiments 1 and 2 to produce an accurate map of the cable shield noise to DARM.

Results and Observations

Using a simple MATLAB script, we combined the results of Experiments 1-3 to obtain the ASD(D) plot found in Figure 14. Additionally, we repeated all three experiments on the

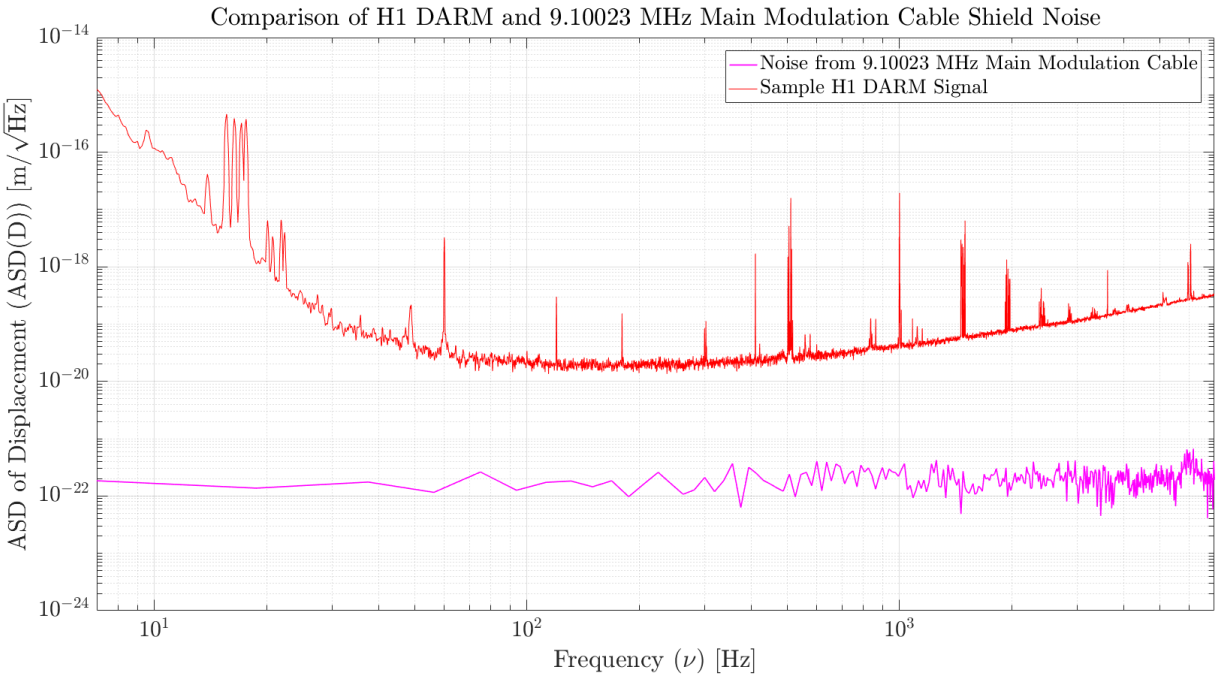

Figure 14: Our final map of the effect of the cable shield noise present on LHO's 9.10023 MHz Main Modulation cable to DARM. Notice that the noise (magenta curve) appears at approximately 10^{-22} m/$\sqrt{\text{Hz}}$, at least two order of magnitudes lower than the current aLIGO noise floor (red curve).

9.10023 MHz Distribution cable, as well as the 45.50115 MHz Auxiliary Modulation cable, the 45.50115 MHz Distribution cable, the 79.4 MHz Return ALS COM VCO cable, the 79.4 MHz Return ALS DIFF VCO cable, and the 79.4 MHz Return PSL VCO cable, obtaining the results in Figures 15 - 20. Figures 14-20 demonstrate that the noise present on the cables under investigation produces a signal on the order of 10^{-22} - 10^{-23} m/$\sqrt{\text{Hz}}$. In fact, this value is only an upper limit of the produced signal due to the noise floor limitations of our spectrum analyzer. As of the writing of this report, the measured DARM of both the Hanford and Livingston observatories appears anywhere from 10^{-15} to 10^{-20} m/$\sqrt{\text{Hz}}$ across the aLIGO observation frequency band. Thus, the effect of the noise on the cables is at least two orders of magnitude lower than the DARM signal across the frequencies that are critical to a successful aLIGO run. From these values, we can conclude that the cable shield noise currently present on every cable tested during our investigation has no negative impact on the the behavior of LHO's interferometer.

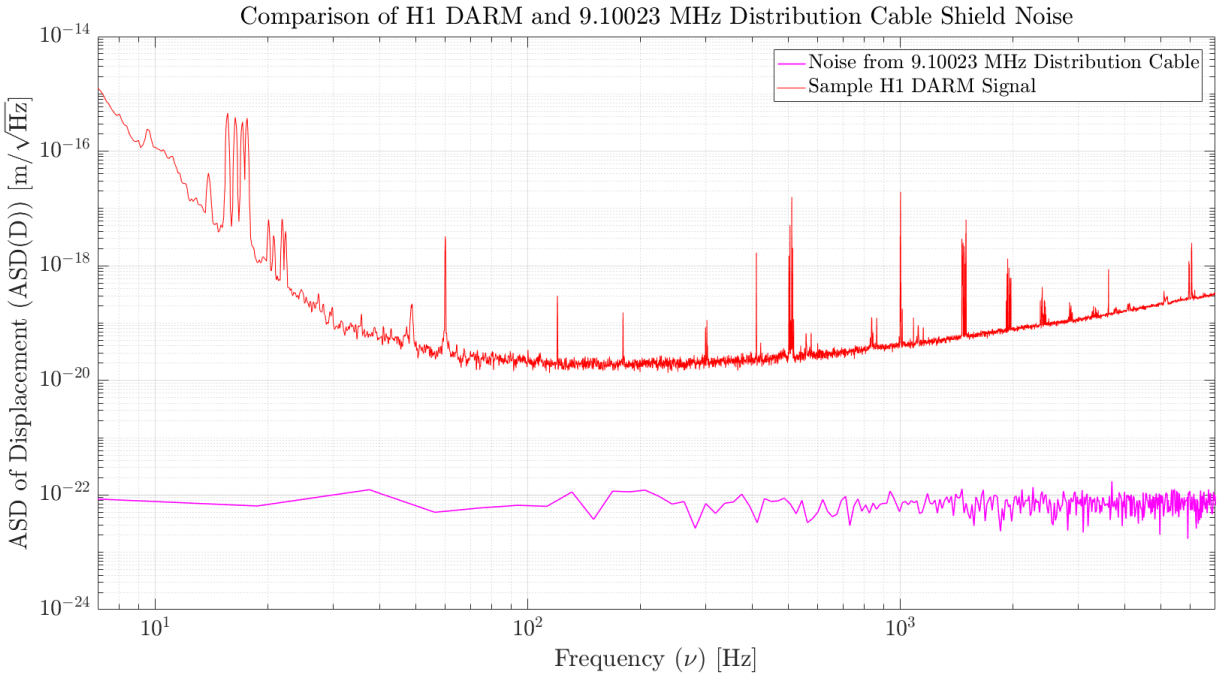

Figure 15: Our final map of the effect of the cable shield noise present on LHO's 9.10023 MHz Distribution cable to DARM. Notice that the noise (magenta curve) appears at approximately 10^{-22} m/$\sqrt{\text{Hz}}$, at least two order of magnitudes lower than the current aLIGO noise floor (red curve).

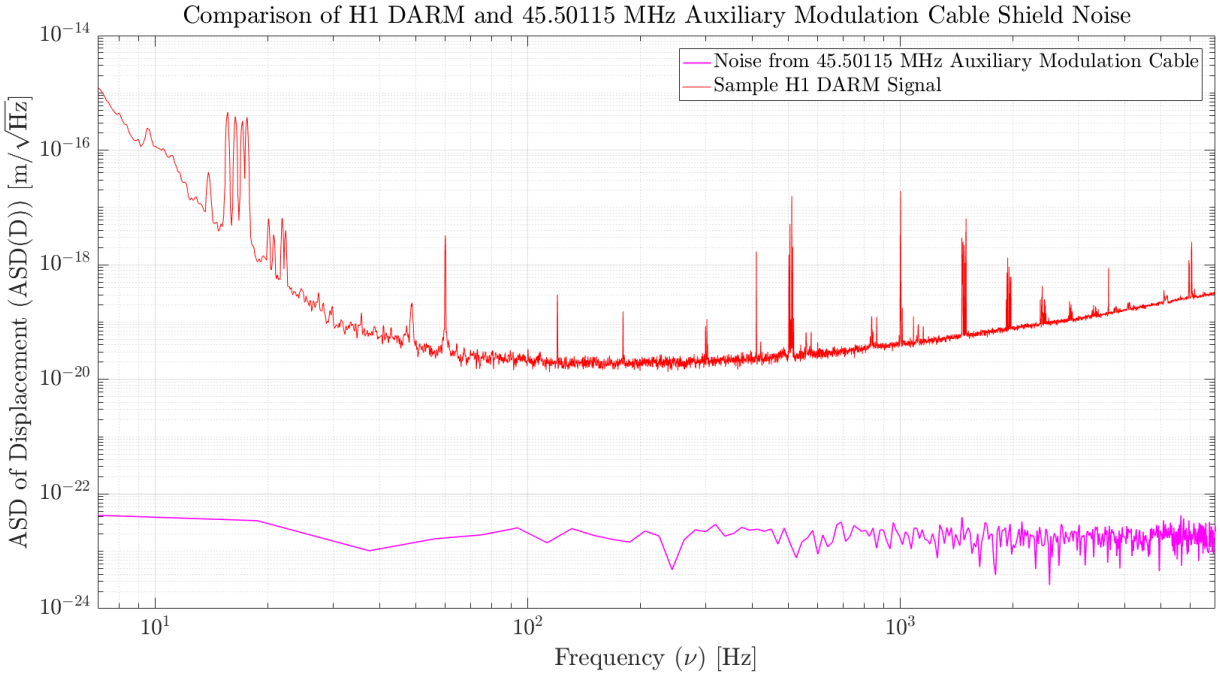

Figure 16: Our final map of the effect of the cable shield noise present on LHO's 45.50115 MHz Auxiliary Modulation cable to DARM. Notice that the noise (magenta curve) appears at approximately 10^{-23} m/$\sqrt{\text{Hz}}$, at least three order of magnitudes lower than the current aLIGO noise floor (red curve).

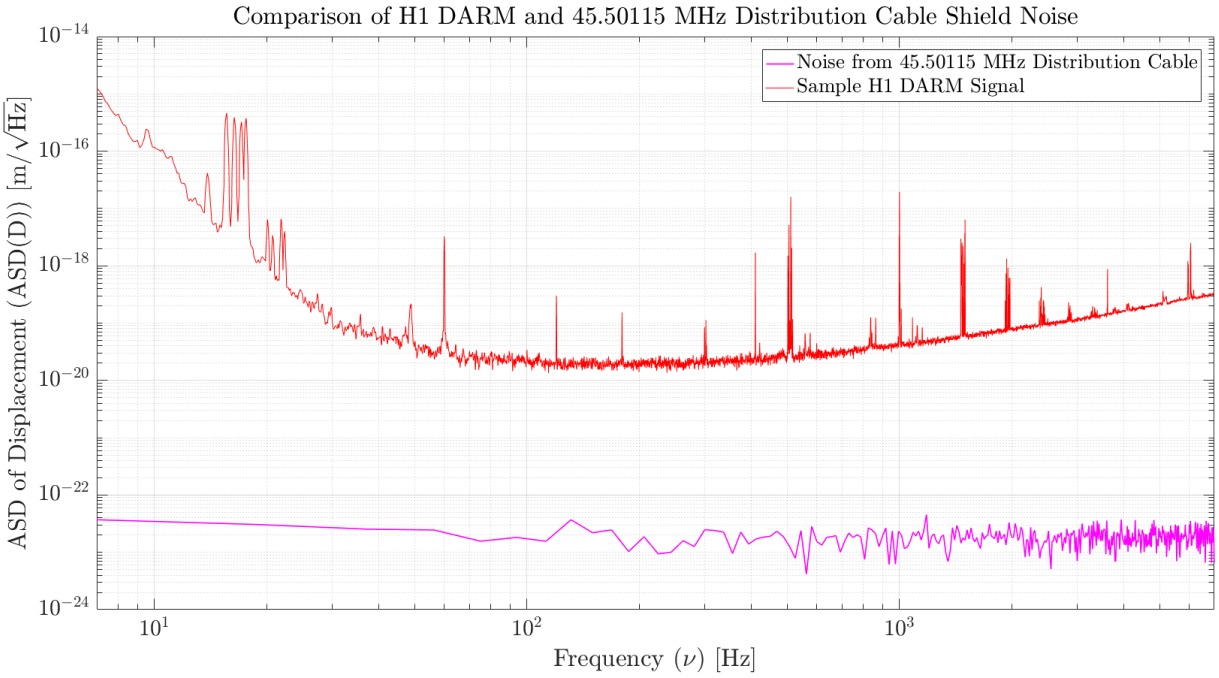

Figure 17: Our final map of the effect of the cable shield noise present on LHO's 45.50115 MHz Distribution cable to DARM. Notice that the noise (magenta curve) appears at approximately 10^{-23} m/$\sqrt{\text{Hz}}$, at least three order of magnitudes lower than the current aLIGO noise floor (red curve).

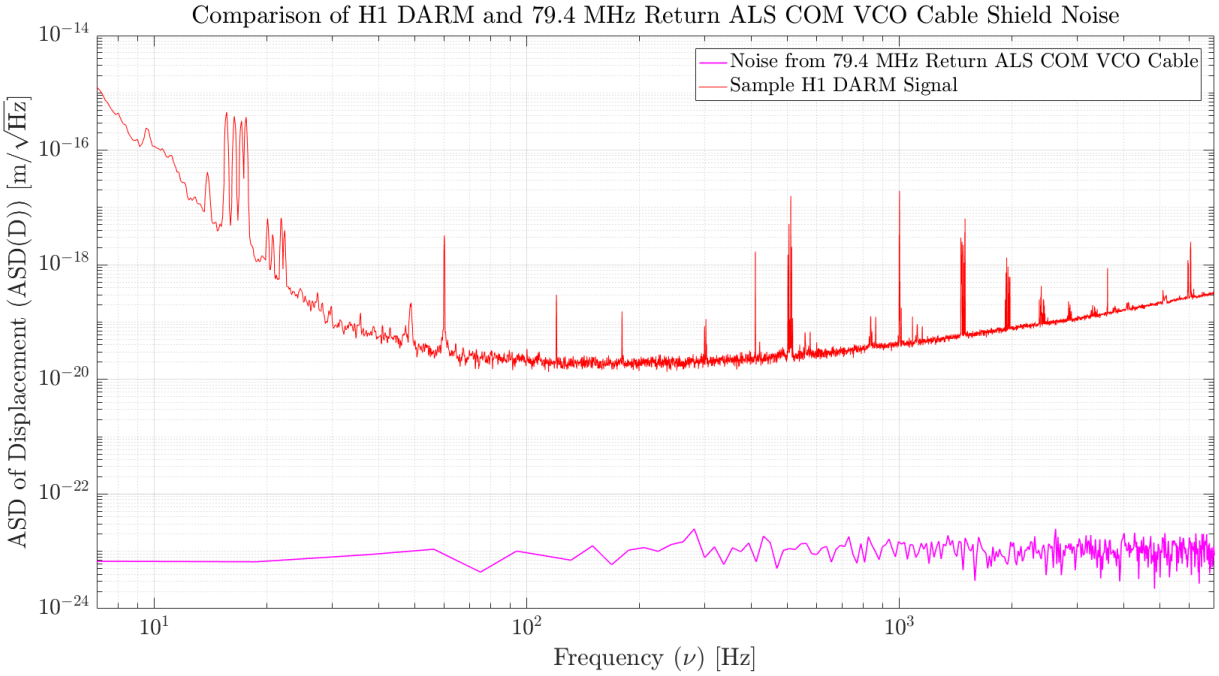

Figure 18: Our final map of the effect of the cable shield noise present on LHO's 79.4 Return ALS COM VCO cable to DARM. Notice that the noise (magenta curve) appears at approximately 10^{-23} m/$\sqrt{\text{Hz}}$, at least three order of magnitudes lower than the current aLIGO noise floor (red curve).

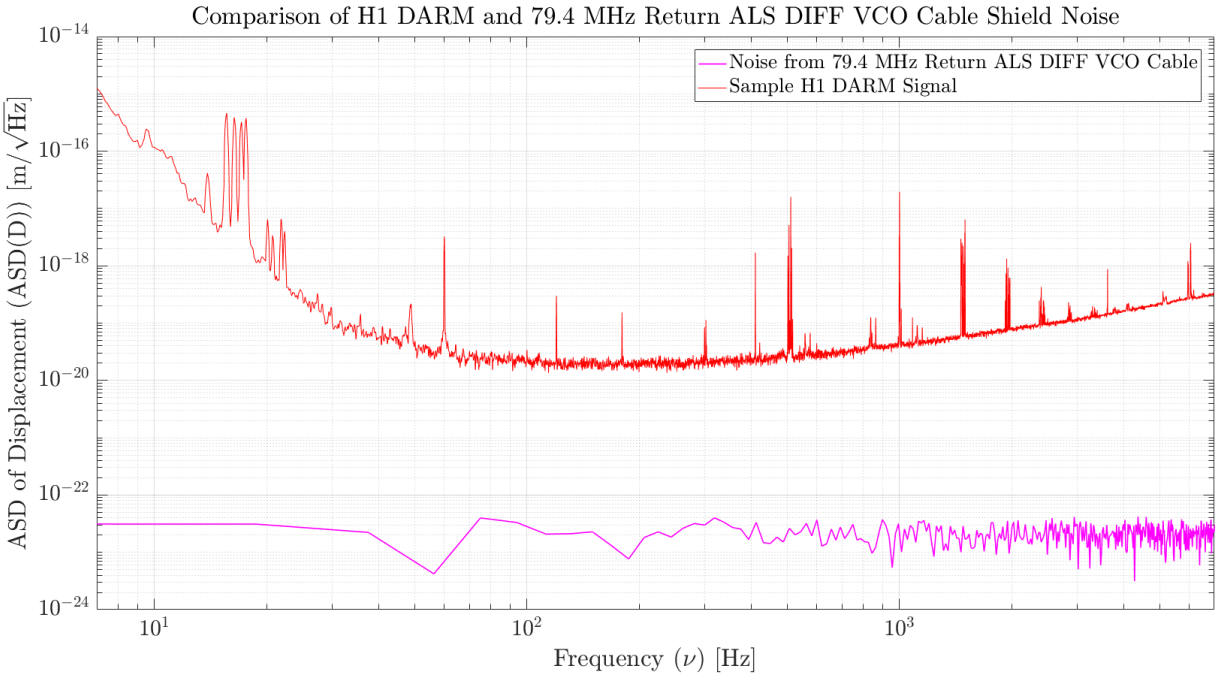

Figure 19: Our final map of the effect of the cable shield noise present on LHO's 79.4 MHz Return ALS DIFF VCO cable to DARM. Notice that the noise (magenta curve) appears at approximately 10^{-23} m/$\sqrt{\text{Hz}}$, at least three order of magnitudes lower than the current aLIGO noise floor (red curve).

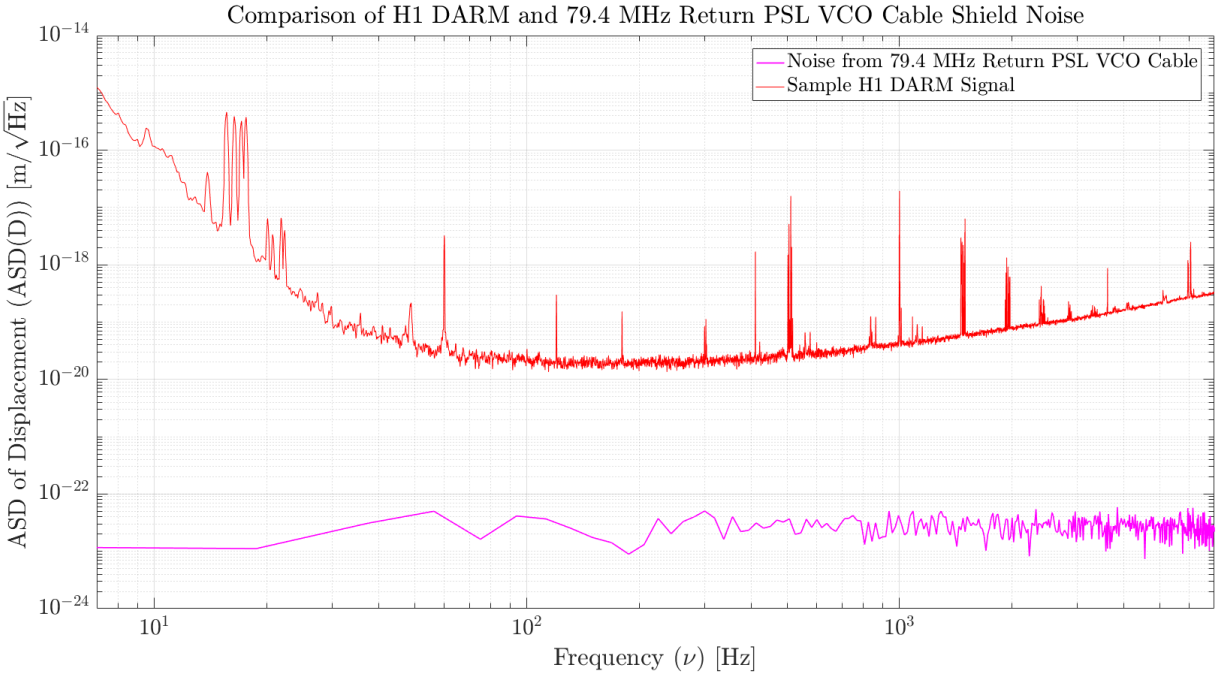

Figure 20: Our final map of the effect of the cable shield noise present on LHO's 79.4 MHz Return PSL VCO cable to DARM. Notice that the noise (magenta curve) appears at approximately 10^{-23} m/$\sqrt{\text{Hz}}$, at least three order of magnitudes lower than the current aLIGO noise floor (red curve).

Model Improvements

We concluded our investigation by critically examining one of the principle assumptions of our sheild noise to DARM mapping model. In Experiment 2, we injected a single RF signal of $V_{inj} = X$ MHZ $+Y$ Hz onto our test cable and then measured the apparent mirror displacement D_{inj} at Y Hz. Together, these two values form the transfer function

$$H(\nu_{inj}) = \frac{D_{inj}}{V_{inj}} = \text{constant}. \tag{7}$$

By using this transfer function in our mapping equation (Equation 5), we assumed that the transfer function between cable noise and the DARM signal is flat. Figure 21 demonstrates this idea. Notice that the green curve, which shows where our transfer function predicts the amplitudes of the injection peaks to fall if we were to repeat our injections at frequencies across the aLIGO DARM spectrum, is simply a horizontal line.

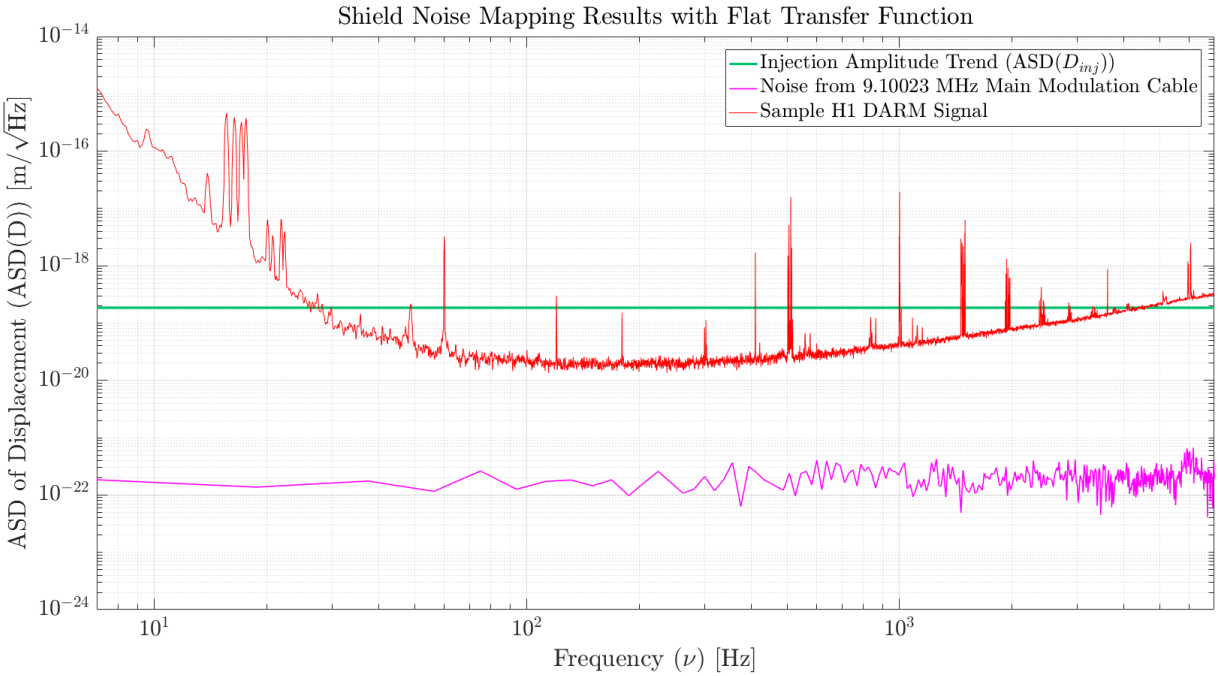

Figure 21: A graph highlighting the flatness of transfer function used to map cable noise to DARM in our initial equation. The green curve shows where our transfer function predicts the injection amplitdes (D_{inj}) to fall across the aLIGO frequency range. The red curve is LHO's DARM signal, and the magenta curve is the calculated effect of shield noise on DARM produced using the flat transfer function.

To test the validity of our flat transfer function assumption, we performed a series of injections onto the 9.10023 MHz Main Modulation cable across several different Y Hz frequency offsets[2]. The red data points in Figure 22 show the transfer function value (D_{inj}/V_{inj}) arising from each injection. The data clearly show that the transfer function does not remain flat; instead, it has a distinct frequency dependence. From inspection of the trend of the data in

[2]The number of injections we were able to perform was limited by access time to the interferometer.

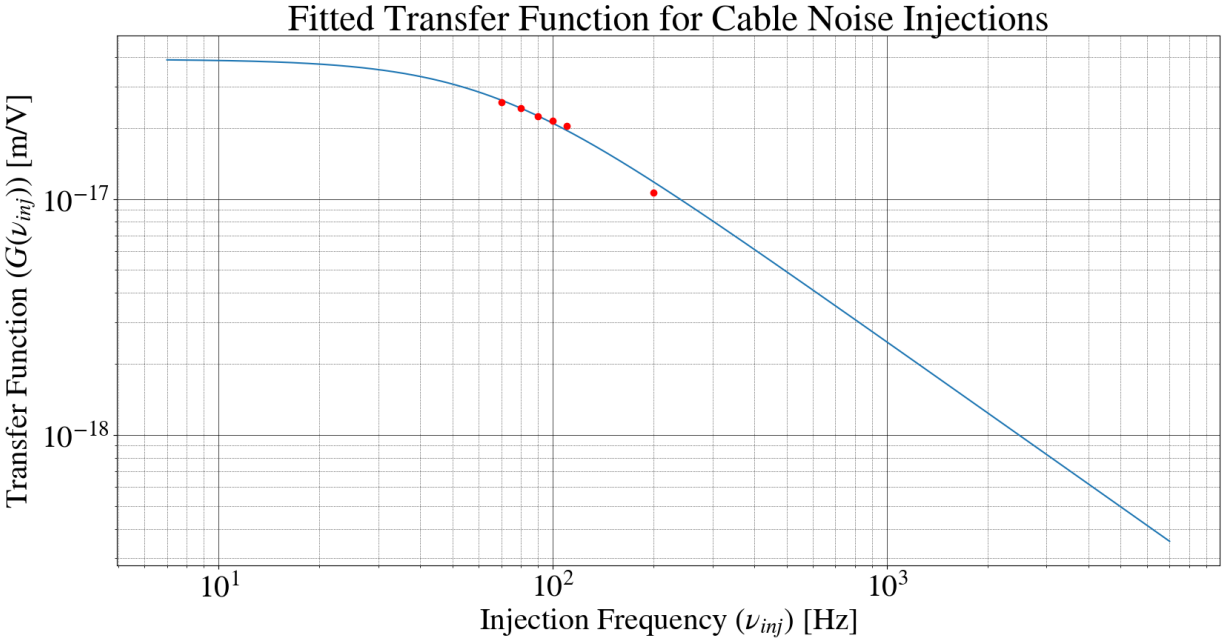

Figure 22: Transfer function values (D_{inj}/V_{inj}) for the 9.10023 MHz Main Modulation cable across several different injection frequencies (red points). The blue curve demonstrates a 1-pole transfer function approach to modeling these values.

log-log space, we hypothesized that the 1-pole transfer function

$$H(\nu_{inj}) = K\frac{1}{1+i\frac{\nu_{inj}}{\nu_0}}, \tag{8}$$

where K and ν_0 are real constants, may appropriately represent the data. By passing this functional form and our collected data to a simple Python curve fitting program, we found $K = 3.91 * 10^{-17}$ $\frac{\text{m}}{\text{V}}$ and $\nu_0 = 63.3$ Hz, allowing us to plot the blue trend line found in Figure 22. Given our limited data set, the fit seemed appropriate, giving us some confidence that we had selected the proper transfer function[3]. Therefore, our shield noise to DARM mapping equation is now

$$\text{ASD}(D) = \frac{1}{ab}\frac{K}{1+i\frac{\nu_{inj}}{\nu_0}}\text{ASD}(V_{probe}). \tag{9}$$

Using this new mapping equation with data from the 9.10023 MHz Main Modulation cable produced the results in Figure 23. Notice that the shield noise is no longer an approximately flat curve at approximately 10^{-22} m/$\sqrt{\text{Hz}}$. Instead, due to the introduction of the 1-pole transfer function, it falls in magnitude at higher frequencies. Overall, however, the shield noise is still at least two orders of magnitude below the current aLIGO noise curve, again suggesting that the sheild noise does not currently have a discernible impact on the output of LHO's interferometer.

[3]Collection of more data points will be necessary to verify that the transfer function, does, in fact, follow this functional form across the entire aLIGO DARM frequency range.

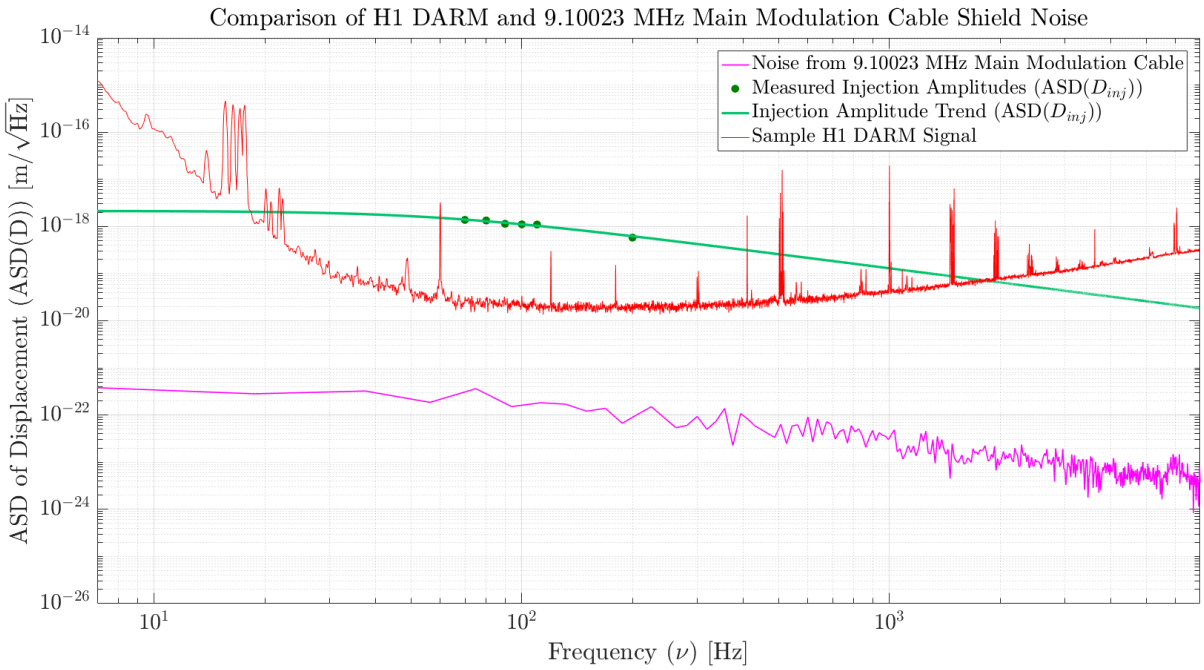

Figure 23: Our final mapping of shield noise to DARM for the 9.10023 MHz Main Modulation Cable. The green points are the injection amplitudes we measured to determine the shape of the transfer function, while the green curve is our hypothesized 1-pole transfer function itself. The magenta curve is the effect of shield noise on DARM. Finally, the red curve is the DARM signal. Notice that while the magenta curve is no longer approximately flat (cf. Figure 21), it is still at least two orders of magnitude below the DARM signal.

Future Work

As we continue our investigation of noise within the RF distribution system at LHO, we intend to carry out three main tasks. First, in order to verify that the transfer function between D_{inj} and V_{inj} truly follows a 1-pole form across the entire aLIGO frequency range, we must perform injections at a wider range of frequency offsets. Second, if we verify the 1-pole behavior, we must perform similar injections on the other cables we considered above in order to produce updated noise curves using the new 1-pole transfer function method. Finally, we would like to use our mapping methodology to determine the of shield noise amplitude that must be present on each cable to induce a measurable impact on DARM. This information will be useful in developing specifications for acceptable levels of cable shield noise in future designs.

References

[1] `https://awiki.ligo-wa.caltech.edu/wiki/RfDesign`

[2] `https://people.ligo-wa.caltech.edu/~daniel.sigg/protel/D0900559-A.pdf`

[3] `https://dcc.ligo.org/DocDB/0063/E1100591/015/E1100591-v15.pdf`

[4] `https://www.commscope.com/catalog/cables/pdf/part/1329/LDF4-50A.pdf`

[5] `https://www.mouser.com/pdfdocs/alphawire-Understanding-Shielded-Cable.pdf`